Surface Science 606 (2012) 186–191

Contents lists available at SciVerse ScienceDirect

Surface Science

journal homepage: www.elsevier.com/locate/susc

Strain effect on diffusion properties of oxygen vacancies in bulk and subsurface of rutile TiO_2

Zhao-Wu Wang, Da-Jun Shu *, Mu Wang *, Nai-Ben Ming

National Laboratory of Solid State Microstructures, Nanjing University, Nanjing 210093, China
Department of Physics, Nanjing University, Nanjing 210093, China

ARTICLE INFO

Article history:
Received 1 August 2011
Accepted 19 September 2011
Available online 29 September 2011

Keywords:
Oxygen vacancy
Strain effect
TiO_2
Diffusion
Density functional calculations

ABSTRACT

The influences of external strain on diffusion properties of the bulk and subsurface oxygen vacancy (OV) in rutile TiO_2 are systematically studied using first-principle calculations. For OVs in bulk, we find that tensile (compressive) strain applied in the [001] direction or isotropically applied in the equivalent [110] and $[1\bar{1}0]$ directions reduces (increases) the energy barriers of diffusion. Anisotropic strain applied in [110] and $[1\bar{1}0]$ increases the energy barriers of diffusion in the two directions. Meanwhile it results in anisotropic diffusion behaviors. Between [110] and $[1\bar{1}0]$, the bulk OV prefers to diffuse along the one in which more compressive or less tensile strain is applied. From subsurface to surface, the most energetically favorable OV pathway is along the [110] rows terminated with the surface bridging oxygen atoms. The diffusion barrier of the OV in the first trilayer is much lower than that of a bulk OV. External in-plane tensile strain can further reduce the energy barrier of the subsurface OV diffusion, and thus help to improve the diffusion of OVs from bulk to surface.

1. Introduction

The point defects in titanium dioxide, including oxygen vacancies and titanium interstitials, contribute excess electrons and play important roles on the applications in a broad variety of fields, such as heterogeneous catalysis, solar cells, gas sensor, photocatalysis, cleaning environment, etc [1–10]. For example, it is well known that oxygen vacancies (OVs) on TiO_2 surfaces are active sites for adsorption and dissociation of molecules [11–14]. Due to the critical roles of point defects, it is possible to modify the properties of TiO_2 by engineering the type and distribution of point defects of TiO_2. For this aim, one should first understand how the external fields influence the formation energies as well as the diffusion properties of point defects.

Strain field is unavoidable especially in fabrication of nanostructures and thin films [15,16]. Recently strain has been taken as a new possible way to facilitate doping, to modify the band structure, and to control the surface reactivity of TiO_2 [17–19]. We have demonstrated that both the formation energies and the diffusion properties of OVs on rutile TiO_2(110) surface can be tuned by the externally applied strain [20,21]. The whole diffusion processes of the defects between bulk and surface under external strain, however, are not yet well-studied although it is necessary for us to understand the strain effects on the distribution of point defects.

The earliest research on the bulk diffusion properties of native point defects in rutile TiO_2, to the best of our knowledge, was reported in 1972 by Iguchi and Yajima [22]. The authors suggested that oxygen vacancies dominate the bulk diffusion according to the isotropic diffusion coefficients. In the 1990's, Henderson reported that titanium interstitials are the major diffusive point defects from the reduced surface to bulk [23], which is believed to be responsible for the bulk-assisted re-oxidation of ion sputtered TiO_2 surface. Recently some first-principle calculations seemed to support this conclusion, showing a lower energy barrier of bulk diffusion of the titanium interstitial than that of the OV (0.37 eV vs. 1.1 eV) [24,25]. However, Wendt et al. reported a larger energy barrier (1.2 eV) of the diffusion of titanium interstitials on subsurface of rutile TiO_2 (110) than in bulk [10,26]. It indicates that the surface Ti interstitial is hindered from diffusing into the bulk although diffusion in bulk is easier than on surface. Oxygen vacancies are energetically more favorable than titanium interstitials, except in a Ti-richer environment [24,27]. However, although surface diffusion of oxygen vacancies has been studied both experimentally and theoretically, there are few studies focusing on the diffusion of OVs from bulk to surface [28–30].

In this paper, we study the diffusion properties of bulk OVs of rutile TiO_2 and the subsurface OVs of TiO_2(110). By investigating the variation of intrinsic stress tensors along the diffusion pathways, strain effects on the OV diffusion properties are predicted and also verified by calculations. For OVs in bulk, we find that tensile strain applied in the [001] direction or isotropically applied in the equivalent [110] and $[1\bar{1}0]$ directions reduces the diffusion barriers, and

* Corresponding authors.
E-mail addresses: djshu@nju.edu.cn (D.-J. Shu), muwang@nju.edu.cn (M. Wang).

0039-6028/$ – see front matter © 2011 Elsevier B.V. All rights reserved.
doi:10.1016/j.susc.2011.09.014

compressive strain increases the barriers. Any anisotropic strain applied in [110] and $[1\bar{1}0]$ increases the energy barrier. Moreover, among [110] and $[1\bar{1}0]$, the bulk OV prefers to diffuse along the one in which more compressive or less tensile strain is applied. From subsurface to surface, the most energetically favorable diffusion pathway of the OV is along the atomic row in [110] terminated with the surface bridging oxygen atoms. The diffusion barrier of the OV in the first trilayer is much lower than that of the bulk OV. Externally applied in-plane tensile strain can reduce the energy barrier of the subsurface OV diffusion. We expect that this work can deepen our understanding about the interaction between external strain and OVs in rutile TiO_2, and demonstrate a possible way to control the diffusion processes using externally applied strain.

2. Computation method

The calculations are based on density functional theory in the PW91 generalized gradient approximation [31], using the Vienna ab initio simulation package code with projector augmented wave pseudopotentials [32,33]. The plane wave cutoff energy is 396 eV. The $2s^2 2p^4$ electrons in O and $3p^6 3d^2 4s^2$ electron in Ti are treated as valence electrons. For studies of the diffusion properties of OV in bulk rutile TiO_2, we have considered different supercells, $(2\times2\times2)$, $(2\times3\times2)$ and $(2\times4\times2)$, with the three basis vectors along $[1\bar{1}0]$ (x), [001] (y) and [110] (z), respectively. Monkhorst-Pack k-points grid [34] of $2\times4\times2$, $2\times3\times2$, and $2\times2\times2$ are used for the supercell of $(2\times2\times2)$, $(2\times3\times2)$ and $(2\times4\times2)$, respectively.

The rutile TiO_2(110) surface is modeled using a (2×2) supercell consisting of a six-trilayer slab and a vacuum with thickness of five trilayers, as shown in Fig. 4(a), the same as in our previous work [20,21]. The O–Ti–O trilayer termination of TiO_2(110) is theoretically predicted to be the most stable one and has also been verified by experiments [6]. Based on purely electrostatic considerations, it is stable because each trilayer is neutral and does not have a dipole moment. Moreover, the number of dangling bonds of titanium on the surface is the same as that of the dangling bonds of oxygen; therefore the surface is autocompensated [35,36]. The relaxation is carried out until all forces on the free ions are converged to 0.01 eV/Å. The bottom two trilayers are fixed during relaxation to mimic the bulk, and no additional atoms are used to saturate the bottom surface. Monkhorst-Pack grid of $2\times4\times1$ is used to sample the k-points. Nudged elastic band (NEB) method is used to find the minimum-energy paths for diffusion of OVs in bulk and subsurface of the rutile TiO_2(110) surface [37].

When viewed from the [001] direction of rutile TiO_2, three types of oxygen sites can be recognized in each trilayer, termed as bridging oxygen (BO), in-plane oxygen (IPO), and subbridging oxygen (SBO) atoms, as shown in Fig. 4(a) for surface. In bulk TiO_2 under natural state, the three types of oxygen atoms are equivalent, so only one kind of OV is created by removing an oxygen atom in the supercell. For surface and subsurface oxygen atoms of TiO_2(110), the atomic surroundings of the oxygen atoms depend both on the type of the oxygen atoms and on the depth of the trilayer. Three types of oxygen vacancies can thus be introduced in each trilayer by removing oxygen atoms of different types, namely bridging OV (BOV), in-plane OV (IPOV) and subbridging OV (SBOV). For reference, we further distinguish the oxygen vacancies by prefixing the trilayer number of the removed oxygen atom. For example, 1-BOV is used to denote the bridging OV in the first trilayer. In all the calculations, only one oxygen is removed in a supercell.

To accurately model the excess electrons from the partially reduced Ti atoms created in the formation of oxygen vacancies, LDA + U method is usually necessary. As for the surface diffusion properties, however, Zhang et al. reported that the vacancy-assisted diffusion of alkoxy species on rutile TiO_2(110) are not dependent upon the nature of the excess electrons [28]. The authors carried out simulations using both standard GGA and LDA + U method, and found that the localization of the excess electrons achieved by employing the LDA + U method yielded almost identical results to those obtained with standard DFT. The possible reason may be found in a recent work where the authors reported that in comparison with GGA, LDA + U method shifts up the conduction-band minimum, while the energy levels of both the valence band and defect state are not affected [38]. It suggests that the errors in the total energy calculations using GGA or LDA + U are transferable. When the diffusion properties are concerned, the on-site Coulomb correction can be canceled when one calculates the energy barrier, which is the energy difference between the saddle point and the stable configuration. Therefore in this work we just use GGA to do the simulations.

3. Oxygen vacancies in a primitive cell of bulk rutile TiO_2

To study the diffusion of OV in bulk rutile TiO_2, we first consider the inequivalent pathways within a primitive cell as shown in the inset of Fig. 1, where we number the oxygen atoms for reference of OVs. The six equivalent oxygen atoms in a primitive cell form an octahedron, with four atoms in the base plane and two atoms in the apex position. By moving an OV in the base plane along [001] (Path I, OV_1–OV_2) or along [110] (Path II, OV_2–OV_3), two inequivalent diffusion paths are obtained. Another different path involves moving an OV in the base plane to the apex position (Path III, OV_3–OV_4).

The energy barriers of the three paths are shown in Fig. 1. For supercell of $(2\times4\times2)$ (solid circles), the barriers are 1.65, 0.61, 1.06 eV for Path I, Path II, and Path III, respectively. The values are consistent with those of charged OVs reported by Iddir [24] (1.77, 0.69 and 1.1 eV for the three paths, respectively). The consistency suggests that the calculation with a neutral supercell is reasonable to describe the OV defects.

In order to check the dependence of diffusion barriers on the OV density, two smaller supercells are considered, namely $(2\times3\times2)$ (solid squares in Fig. 1) and $(2\times2\times2)$ (solid triangles). The size of one unit cell along the $[1\bar{1}0]$ and [110] directions is more than two times of the one along [001]. It has been reported that two unit cells along the $[1\bar{1}0]$ and [110] directions are large enough to eliminate the cross-row interaction of oxygen vacancies [30]. Therefore we only vary the lattice number of the supercell in the [001] direction. We find that the energy barrier of Path I is the highest for all studied supercells. For supercell of $(2\times3\times2)$, the energy barrier of Path III almost remains the same as that in $(2\times4\times2)$. The barrier of Path II increases but is still lower than that of Path III. When the density of OVs increases as the supercell decreases to $(2\times2\times2)$, the energy barrier of Path II increases further; meanwhile the barrier of Path III

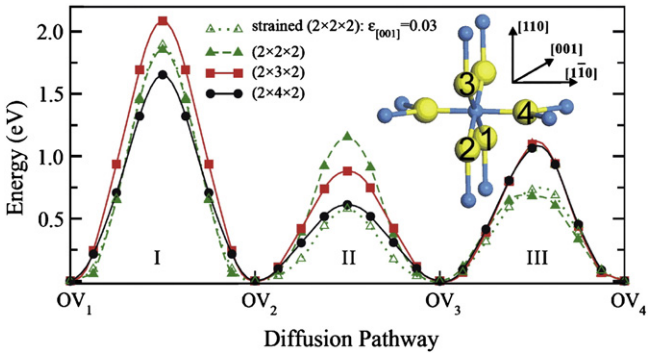

Fig. 1. Energy profiles of OV pathways within the primitive cell of rutile TiO_2 using different size of supercell, namely $(2\times2\times2)$, $(2\times3\times2)$ and $(2\times4\times2)$. The inset shows the schematic of a primitive cell. Large light spheres and small dark spheres denote the O and Ti atoms, respectively (the same below). The numbers label different oxygen atoms in order for reference of OVs. The notations I, II and III correspond to the paths from OV_1 to OV_2, from OV_2 to OV_3 and from OV_3 to OV_4, respectively.

decreases and becomes the lowest. It suggests that the interaction between OVs in the [001] direction facilitates the diffusion of OVs along Path III, but suppresses the diffusion along Path II. It is understandable because in the saddle point of Path II, the moving oxygen atom sits in the middle of OV_2 and OV_3, which is expected to induce compressive inner stress in the [001] direction. Higher OV density in the [001] direction induces larger compressive stress, thus making Path II energetically unfavorable in supercell of $(2\times2\times2)$.

The inner stress tensors accompanied with the OV diffusion in the bulk TiO_2 is calculated to further understand the diffusion processes. To distinguish with the surface stress which is usually denoted as σ, we denote the inner stress as P. From Fig. 2, we can see that the stress tensors $P_{[001]}$ and $P_{[110]}$ in the saddle points of Path II are most notable. Increasing OV density in the [001] direction induces larger compressive stress in the saddle point of Path II in the [001] and [110] directions, as expected.

Energetically since tensile strain can partly counteract the effect of compressive stress which is induced in the saddle point, it is expected to favor Path II of OVs even for large OV density. To demonstrate the influence of the OV density on the energy barrier in term of inner stress, we show in Fig. 1 the calculated energy barrier of the three diffusion paths in $(2\times2\times2)$ under 3% externally applied tensile strain along the [001] direction (triangles, dashed line). It is evident that the energy barrier of Path II decreases to almost the same value in $(2\times4\times2)$, while Path I and Path III are almost unaffected.

4. Strain effect on bulk diffusion of OVs in rutile TiO_2

Now we analyze the anisotropy of diffusion properties of bulk, and study the influence of external strain according to the inner stress tensor along the diffusion paths. The supercell of $(2\times4\times2)$ is considered in order to mimic the nearly isolated OVs. Due to the largest barrier of Path I, direct migration along [001] can be avoided by using a combination of Path III. Therefore we only consider the diffusion along the $[1\bar{1}0]$ and [110] directions, *i.e.*, OV_1–OV_2–OV_3–OV_4 and OV_1–OV_2'–OV_3'–OV_4', respectively, as denoted in Fig. 3(a). In non-strained state, or when non-zero but isotropic strain is applied in the $[1\bar{1}0]$ and [110] directions, all the bulk oxygen atoms and thus OVs are equivalent (EQ OVs for short in Fig. 3(b)). In this case, it is obvious that the diffusion properties in the two directions are also equivalent.

When no strain is applied, the global barrier of the diffusion in the $[1\bar{1}0]$ or [110] direction is limited by the barrier of Path III in a primitive cell, *i.e.*, OV_2–OV_3 or OV_1–OV_2' as shown in Fig. 3(a). When external strain is applied, we have demonstrated in our previous work that the strain effect on the surface OV diffusion can be predicted according to the surface stress profile along the diffusion pathways [21],

$$E^i = E_0^i + A_L \Delta\sigma^i \epsilon, \tag{1}$$

where E^i and σ^i are the energy and the intrinsic surface stress tensors at the ith configuration along the diffusion pathway, respectively. E_0^i is the energy when no strain is applied, and A_L is the surface area in unstrained state. For bulk system, it is easy to modify this formula by replacing the surface stress tensor σ_i with the inner stress tensor P_i,

$$E^i = E_0^i + V_L \Delta P^i \epsilon, \tag{2}$$

where V_L is the volume in unstrained state. Eq. (2) can be verified by considering the three paths in a primitive cell with supercell of $(2\times2\times2)$ under strain of $\epsilon_{[001]}=0.03$. We find that the calculated energy barriers (dotted curve in Fig. 1) are consistent with the predicted values according to Eq. (2), which demonstrates that Eq. (2) can be directly used to study the interaction of external strain and the diffusion properties of OVs in bulk rutile TiO_2.

Substituting the calculated stress tensors into Eq. (2), we obtain the energy profiles of the OV diffusing along the two directions in different strained states, as shown in Fig. 3. When the strain along [110] and $[1\bar{1}0]$ is isotropic, only diffusion pathways along $[1\bar{1}0]$ is shown in Fig. 3(b), since the [110] and $[1\bar{1}0]$ directions are equivalent. In this case, we find that the tensile strain in the [001] direction or biaxially along the equivalent [110] and $[1\bar{1}0]$ directions reduces the global energy barrier, while compressive strain increases the barrier.

The global barriers both along [110] and along $[1\bar{1}0]$ increase whenever the strain along [110] and $[1\bar{1}0]$ is different, as can be seen from Fig. 3(c–f). It means that anisotropic strain applied in [110] and $[1\bar{1}0]$ always suppresses the bulk OV diffusion. It is not strange if one notes that any anisotropic strain in the two directions will separate the otherwise equivalent bulk oxygen atoms into two different types with different formation energies, which increases the energy barriers of OV diffusion in the two directions.

Besides, anisotropic bulk diffusion along the [110] and $[1\bar{1}0]$ directions is expected under anisotropic strain state. When tensile external strain is applied in $[1\bar{1}0]$ direction, the energy barrier in the [110] direction becomes lower than that in the $[1\bar{1}0]$ direction, which means diffusion of OV along the [110] direction dominates. When compressive external strain is applied in the $[1\bar{1}0]$ direction, the more favorable diffusion pathway is along the $[1\bar{1}0]$ direction. After systematic comparison, the conclusion can be drawn that, among $[1\bar{1}0]$ and [110], the bulk OV prefers to diffuse along the direction in which more compressive or less tensile strain is applied. It is interesting for real applications. For instance, in TiO_2 which is epitaxially grown on a foreign substrate with TiO_2 (110) as the interface, the OVs in bulk prefer to diffuse in perpendicular or in parallel to the interface, depending on whether the misfit strain is tensile or compressive.

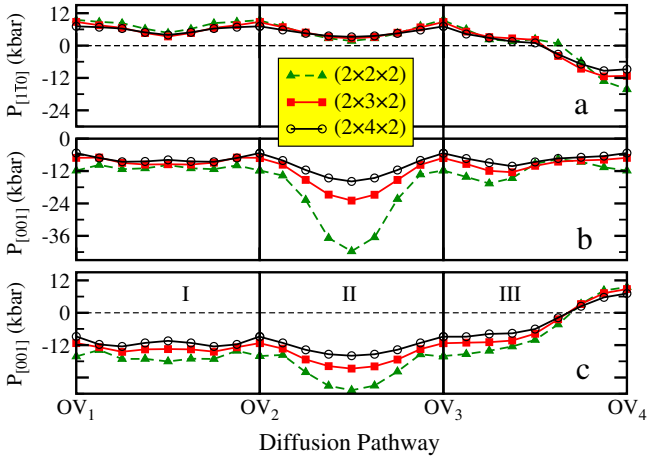

Fig. 2. The variation of inner stress tensors in directions of $[1\bar{1}0]$ ($P_{[1\bar{1}0]}$), [001] ($P_{[001]}$) and [110] ($P_{[110]}$), along the OV pathways within a primitive cell of bulk rutile TiO_2. The bulk is modeled with supercell of $(2\times2\times2)$, $(2\times3\times2)$ and $(2\times4\times2)$. Notations I, II and III stand for Path I, Path II and Path III respectively.

5. Diffusion of subsurface OVs of TiO_2(110)

Since the formation energy of OVs in the third trilayer is already approaching that in the bulk, we expect that the diffusion of the subsurface OVs can give us a picture of the diffusion of OV between the bulk and the surface [20]. In order to mimic the surface using a moderate time-consuming setup, a surface supercell of (2×2) is used. The density of the introduced oxygen vacancy density is therefore 1/4, with 1/2 (removing one every two oxygen atoms) along both the $[1\bar{1}0]$ and the [001] directions. Interaction between neighboring OVs in [001] may have influences on the diffusion properties of OVs. Fortunately, according to the discussion in Section 3, tensile strain

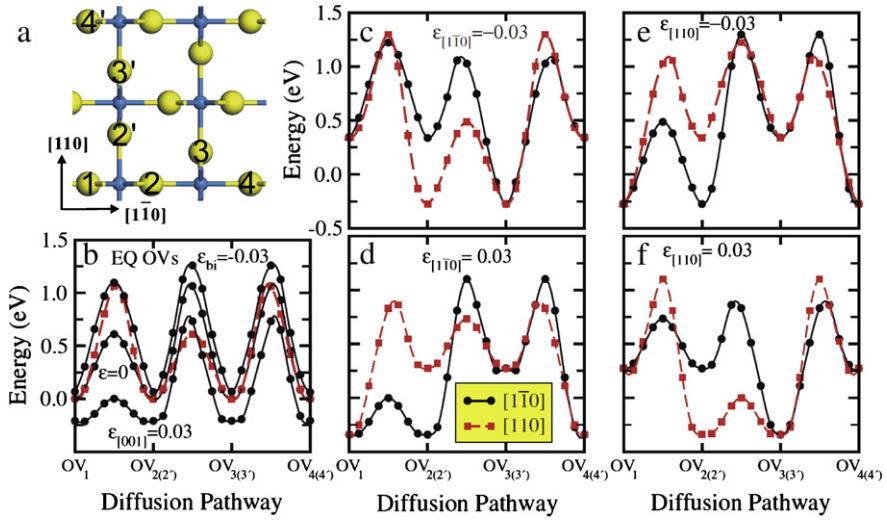

Fig. 3. (a) Schematic of bulk OV diffusion along the [110] and [$1\bar{1}0$] directions in rutile TiO_2. The numbers label different oxygen atom sites for reference in (b–f). (b–f) The energy profiles of OV diffusion in rutile TiO_2, when isotropic strain (b) or anisotropic strain applied in directions along [$1\bar{1}0$] (c and d) and [110] (e and f).

can partly cancel out the effect of the compressive stress. Considering the tensile nature of the surface stress of TiO_2(110) [20,21,39], the (2×2) supercell is reasonable to study the diffusion properties of subsurface OVs while keeping the computer demands moderate.

The subsurface diffusion is complicated since there are lots of possible diffusion pathways of subsurface OVs. This situation can be clarified by grouping the atoms as shown in Fig. 4(a). When viewed from the [110] direction, the subsurface titanium atoms form Ti rows, and

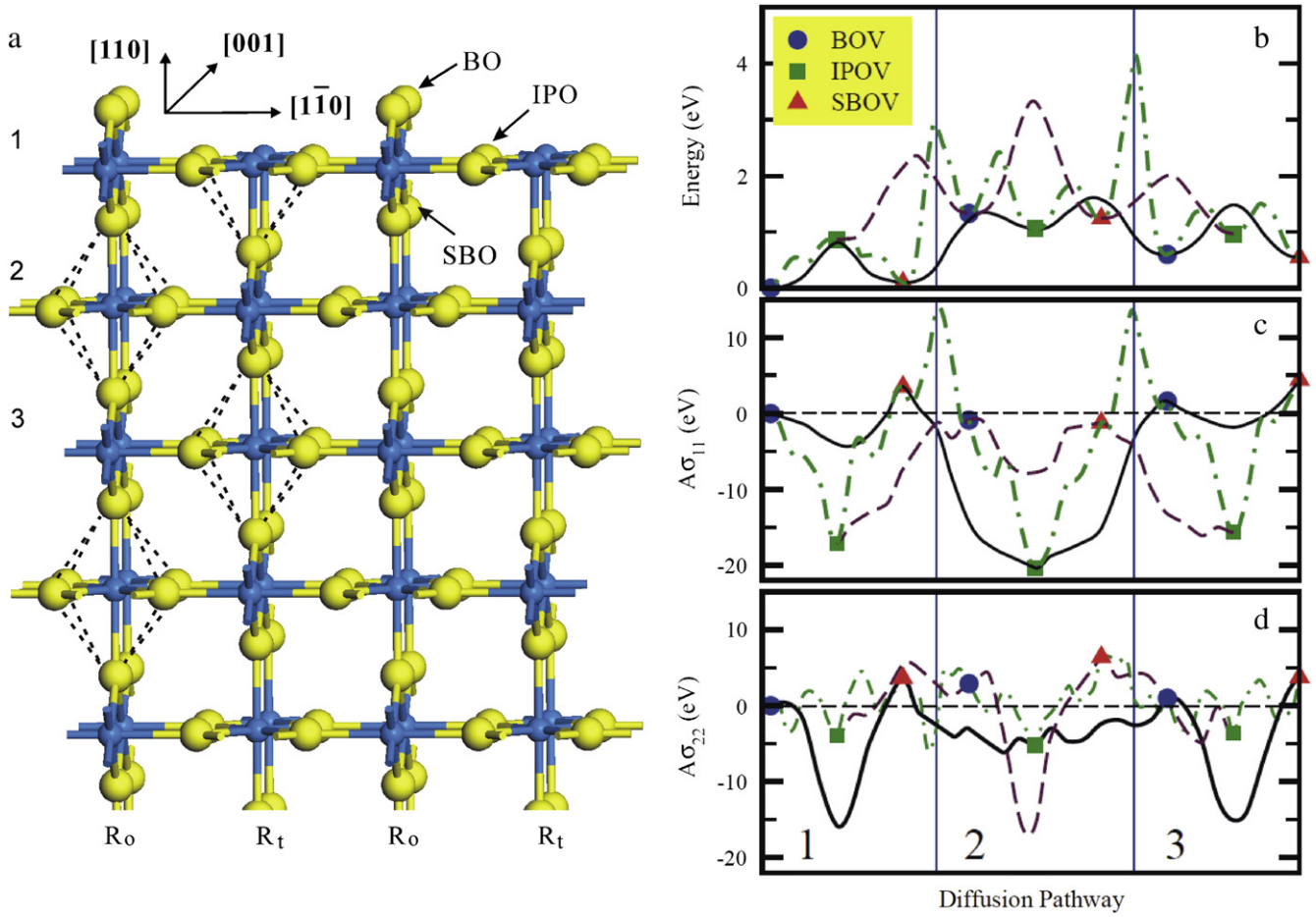

Fig. 4. (a) Schematic of the rutile TiO_2(110) surface. The bridging oxygen (BO), the subbridging oxygen (SBO) and the in-plane oxygen (IPO) atoms are indicated by the arrows. R_o and R_t denote the atomic rows in [110] direction, with surface terminated by the bridging oxygen atoms or the five-coordinated titanium atoms, respectively. (b) The energy profiles of the subsurface OV diffusion. (c) and (d) are the variation of the surface stress tensor along the diffusion pathways. The subscripts 11 and 22 denote the directions along [$1\bar{1}0$] and [001], respectively (same below). Both the energies and the surface stress tensors are given in reference to the values of the bridging OV in the first trilayer (1-BOV). The numbers 1–3 on (a) and (d) denote the trilayer number.

the rows can be categorized into two groups. In one group, the atomic [110] rows are terminated with the two-coordinated bridging oxygen atoms (labeled as R^o hereafter for reference), and in the other group the rows are terminated with the five-coordinated titanium atoms on the surface (R_t). For easier understanding, the oxygen atoms can be regarded as in octahedrons with the long axis along the [110] direction. Thus the in-plane oxygen atoms form the base plane of the octahedrons, and the (sub)bridging oxygen atoms are in the apices. The octahedrons are periodically aligned in the [110] rows and connected with titanium atoms which are not contained in the octahedrons. Note that we do not completely follow the definition of octahedrons in bulk because we intentionally ignore the sets of octahedrons with the long axis along $[1\bar{1}0]$ for clarify.

The energy profiles of all the possible diffusion pathways of the OVs in the outermost three trilayers are calculated using NEB methods, as shown in Fig. 4(b). The solid and dashed curves display the pathways of the OV along R_o and along R_t, respectively. The dot–dashed curve guides the paths of OV hopping between R_o and R_t. First we can see that the path between SBOV and BOV in neighboring trilayers (thus in neighboring R_o and R_t) is of very high energy barrier and thus are impossible to occur. The similar path in bulk is also of high energy barrier according to our calculations (not shown). The energy barrier between SBOV and BOV in the same trilayer is lower in R_o than that in R_t. This difference is understandable by recalling that the transition state of this path in bulk induces extra compressive stress in the [110] direction, as shown in Fig. 2(c). Since surface relaxation leads local tensile strain in R_o and compressive strain in R_t along [110] [6], compared with that in bulk, the barrier between the subsurface SBOV and BOV within the same trilayer becomes lower in R_o and higher in R_t. Additionally, partly due to the tensile nature of the surface stress [20,21,39], the energy barrier in the first trilayer from SBOV is smaller to BOV than to IPOV, as in bulk with a larger supercell. It justifies the reasonability of using $(2\times2\times2)$ supercell to give the correct subsurface diffusion properties with moderate the calculation demands.

According to the calculations, we can find the favorable diffusion pathway of any specific subsurface OV by comparing the energy barrier of the possible paths. For clarity, we display the calculated energy barriers between different initial OVs and final OVs in Table 1. In brackets we denote the Ti atomic row to which the OV belongs. From subsurface to surface, it is clear that OVs in R_o tend to diffuse within the same row, but in R_t they prefer to hop to the neighboring R_o unless the hop occurs between SBOV and BOV. Therefore globally the best energetically favorable pathway of the subsurface is along R_o, as shown by the solid curve in Fig. 4(b). It is worthy to note that the highest barrier occurs when the subsurface OV crosses the second trilayer. Thus the 3-BOV prefers to diffuse downwards into bulk, whereas the 1-SBOV prefers to hop to the surface.

6. Strain effect on diffusion of subsurface OVs

In order to study the strain effect on the diffusion properties of subsurface OVs, we calculate the variation of the surface stress along the diffusion pathways, as shown in Fig. 4(c) and (d). In Table 1 we also list the difference between the stress tensor of the saddle points and that in the initial states, $\Delta\sigma$, for all the possible pathways.

From Fig. 4(c) and (d), we can see that the stress of IPOVs is always the lowest for the corresponding pathways. It is more clearly shown in Table 1 by the positive $\Delta\sigma_{11}$ and $\Delta\sigma_{22}$ (bolded fonts) along the pathways initiated from the IPOV. Therefore compressive external strain can reduce the energy barrier of the diffusion from IPOVs to other OVs. Besides, as indicated by the other positive $\Delta\sigma_{11}$ shown in bolded fonts in Table 1, compressive strain applied in $[1\bar{1}0]$ is expected to lower the energy barriers of diffusion between the SBOV and the BOV in neighboring trilayers. In the [001] direction, instead, compressive strain can lower the barrier of the other two paths involving BOV and IPOV, from 2-BOV to 1-IPOV and from 3-BOV to 3-IPOV. Along all the other pathways, the transition states are most compressive along both [001] and $[1\bar{1}0]$ (negative $\Delta\sigma_{11}$ and $\Delta\sigma_{22}$), which suggests that tensile applied strain can facilitate the diffusion of subsurface OVs.

Table 1
Energy barriers of the subsurface OV diffusion of rutile TiO_2(110), including upwards to surface (up) and downwards into deeper layers (down). Also shown are the differences of the surface stress tensor between the corresponding saddle points and the initial states, $\Delta\sigma$. A is the surface area. The values are in unit of eV. The positive $\Delta\sigma$ are given in bold fonts for distinguishing.

Initial state	Final state	Up/down	E^b	$A\Delta\sigma_{11}$	$A\Delta\sigma_{22}$
1-SBOV (R_o)	1-BOV (R_o)	u	0.71	−7.53	−19.4
	1-IPOV (R_t)	u	0.78	−16.02	−3.46
	2-IPOV (R_o)	d	1.25	−20.56	−8.29
	2-BOV (R_t)	d	2.82	**9.85**	−6.85
2-BOV (R_t)	1-IPOV (R_t)	u	1.00	−3.19	**1.93**
	1-SBOV (R_o)	u	1.59	**14.23**	−6.12
	2-IPOV (R_o)	d	1.00	−4.95	−1.29
	2-SBOV (R_t)	d	1.98	−6.91	−18.71
2-IPOV (R_o)	1-SBOV (R_o)	u	0.28	**3.29**	**0.55**
	2-BOV (R_t)	u	1.27	**14.52**	**6.82**
	3-BOV (R_o)	d	0.51	**5.22**	**2.82**
	2-SBOV (R_t)	d	0.81	**11.63**	**5.86**
2-SBOV (R_t)	2-IPOV (R_o)	u	0.63	−7.49	−5.74
	2-BOV (R_t)	u	2.07	−6.56	−22.2
	3-IPOV (R_t)	d	0.76	−12.01	−5.86
	3-BOV (R_o)	d	2.83	**14.35**	−5.62
3-BOV (R_o)	2-IPOV (R_o)	u	0.98	−16.75	−3.36
	2-SBOV (R_t)	u	3.47	**11.5**	−0.20
	3-SBOV (R_o)	d	0.88	−3.46	−16.06
	3-IPOV (R_t)	d	0.82	−5.94	**0.85**
3-IPOV (R_t)	3-BOV (R_o)	u	0.45	**11.3**	**5.47**
	2-SBOV (R_t)	u	1.04	**2.38**	**4.18**
	3-SBOV (R_o)	d	0.51	**13.62**	**6.97**
3-SBOV (R_o)	3-BOV (R_o)	u	0.93	−6.26	−18.85
	3-IPOV (R_t)	u	0.93	−6.42	−0.44

Since the influence of the external strain on the energy barriers depends on the specific pathways, the relative order of preferability of diffusion pathways may be changed by the external strain. Substituting the energy and surface stress of each configuration along the diffusion pathways into Eq. (1), we calculate and replot the energy profiles of the diffusion paths, as shown in Fig. 5. We can see that the diffusion of 3-SBOV to 3-BOV is more likely to occur mediated by the 3-IPOV when 2% compressive strain is applied along the [001] direction (Fig. 5(c)), compared to the direct hoping way when tensile strain is applied (Fig. 5(d)).

The global energy barrier of OV from subsurface to surface decreases with increasing tensile strain. Especially when the strain along $[1\bar{1}0]$ is 2%, all the subsurface OVs become easier to hop to surface than to bulk (Fig. 5(b)). It suggests that tensile strain can be applied to improve the diffusion of OVs in bulk to surface. As an example of demonstration we carry out the first-principle calculation of the pathway from 2-SBOV to 2-IPOV under external strain of $\pm1\%$ and $\pm2\%$. The results show that the first-principle calculations are consistent with the prediction within the considered magnitude of the external strain.

7. Conclusions

In summary, by calculating the variation of the stress tensors along the diffusion pathways, the diffusion properties of the oxygen vacancy in bulk of rutile TiO_2 and subsurface of rutile TiO_2(110) under strained states are studied using first-principle calculations. For the OV in bulk, we find that tensile (compressive) strain applied in the [001] direction or isotropically applied in the equivalent [110] and $[1\bar{1}0]$ directions reduces (increases) the energy barrier of diffusion. Anisotropic strain applied in [110] and $[1\bar{1}0]$ increases the

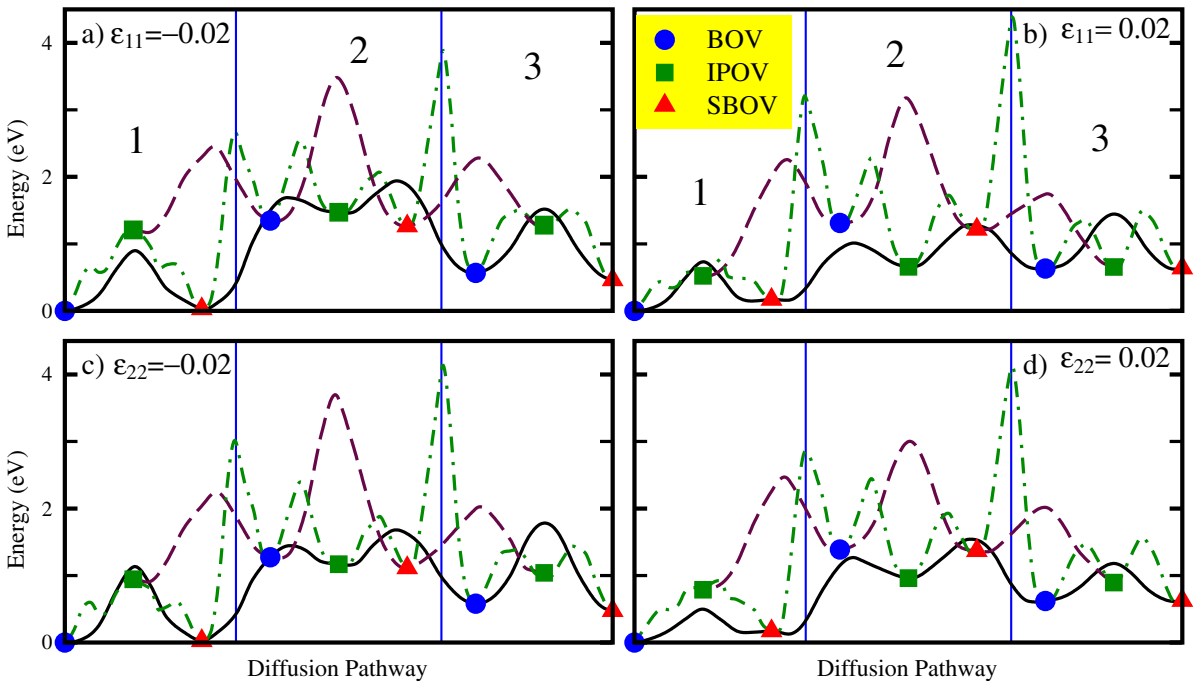

Fig. 5. The energy profiles of the subsurface OV diffusion under different states of applied strain. In the upper and lower panels, the strain is applied in the $[1\bar{1}0]$ and [001] directions, respectively.

energy barrier, and also results in anisotropic diffusion behaviors along the two otherwise equivalent directions. Among [110] and $[1\bar{1}0]$, the bulk OV prefers to diffuse along the direction in which more compressive or less tensile strain is applied. For a subsurface OV, the most energetically favorable diffusion pathway is along the [110] rows which are terminated with the surface bridging oxygen atoms. The diffusion barrier of OV on the surface is much lower than that of a bulk OV. Externally applied tensile strain can reduce the energy barrier of the subsurface OV diffusion, and help to improve the diffusion of OVs in bulk to surface. We believe that external strain is a good way of tuning the diffusion behaviors of OVs in bulk and subsurface, and thus can be used to engineer the practical physical and chemical properties of TiO_2.

Acknowledgements

The numerical calculations have been carried out at the High Performance Computing Center of Nanjing University and the Shanghai Supercomputer Center. This work was supported by NSF of China (under Grant Nos. 10974079, 11174123, and 11034005) and Jiangsu Province (under Grant No. BK2008012), MOE of China (under Grant No. NCET-09-0461) and MOST of China (under Grant Nos. 2010CB630705 and 2012CB921502).

References

[1] R. Asahi, T. Morikawa, T. Ohwaki, K. Aoki, Y. Taga, Science 293 (2001) 269.
[2] C.T. Campbell, S.C. Parker, D.E. Starr, Science 298 (2002) 811.
[3] M. Gratzel, Nature 414 (2001) 338.
[4] O. Bikondoa, C.L. Pang, R. Ithnin, C.A. Muryn, H. Onishi, G. Thornton, Nat. Mater. 5 (2006) 189.
[5] G. Lu, A. Linsebigler, J.T. Yates, J. Phys. Chem. 99 (1995) 7626.
[6] U. Diebold, Surf. Sci. Rep. 48 (2003) 53.
[7] J. He, R.K. Behera, W.M. Finnis, X. Li, E.C. Dickey, S.R. Phillpot, S.B. Sinnott, Acta Materialia 55 (2007) 4325.
[8] S. Wendt, J. Matthiesen, R. Schaub, E.K. Vestergaard, E. Laegsgaard, F. Besenbacher, B. Hammer, Phys. Rev. Lett. 96 (2006) 066107.
[9] K. Park, M. Pan, V. Meunier, E.W. Plummer, Phys. Rev. B 75 (2007) 24515.
[10] S. Wendt, P.T. Sprunger, E. Lira, G.K.H. Madsen, Z.S. Li, J.O. Hansen, J. Matthiesen, A. Blekinge-Rasmussen, E. Laegsgaard, B. Hammer, et al., Science 320 (2008) 1755.
[11] W.S. Epling, C.H.F. Peden, M.A. Henderson, U. Diebold, Surf. Sci. 412–13 (1998) 333.
[12] M.A. Henderson, Surf. Sci. 400 (1998) 203.
[13] C.L. Pang, R. Lindsay, G. Thornton, Chem. Soc. Rev. 37 (2008) 2328.
[14] K. Onda, B. Li, J. Zhao, K.D. Jordan, J.L. Yang, H. Petek, Science 308 (2005) 1154.
[15] B. Yang, F. Liu, M.G. Lagally, Phys. Rev. Lett. 92 (2004) 025502.
[16] G.H. Lu, M. Cuma, F. Liu, Phys. Rev. B 72 (2005) 125415.
[17] W.J. Yin, S.Y. Chen, J.H. Yang, X.G. Gong, Y.F. Yan, S.H. Wei, Appl. Phys. Lett. 96 (2010) 221901.
[18] P.D. Mitev, K. Hermansson, B. Montanari, K. Refson, Phys. Rev. B 81 (2010) 134303.
[19] L. Thulin, J. Guerra, Phys. Rev. B 77 (2008) 195112.
[20] D.J. Shu, S.T. Ge, M. Wang, N.B. Ming, Phys. Rev. Lett. 101 (2008) 116102.
[21] Z.W. Wang, D.J. Shu, M. Wang, N.B. Ming, Phys. Rev. B 82 (2010) 165309.
[22] E. Iguchi, K. Yajima, J. Phys. Soc. Jpn. 32 (1972) 1415.
[23] M.A. Henderson, Surf. Sci. 419 (1999) 174.
[24] H. Iddir, S. ogut, P. Zapol, N.D. Browning, Phys. Rev. B 75 (2007) 073203.
[25] A.M. Asaduzzaman, P. Kruger, J. Phys. Chem. C 114 (2010) 19649.
[26] Z. Zhang, J. Lee, J.T. Yates, R. Bechstein, E. Lira, J.O. Hansen, S. Wendt, F. Besenbacher, J. Phys. Chem. C 114 (2010) 3059.
[27] E. Cho, S. Han, H.-S. Ahn, K.-R. Lee, S. Kim, C. Hwang, Phys. Rev. B 73 (2006) 193202.
[28] Z. Zhang, Q. Ge, S.C. Li, B.D. Kay, J.M. White, Z. Dohnalek, Phys. Rev. Lett. 99 (2007) 126105.
[29] X. Cui, B. Wang, Z. Wang, T. Huang, Y. Zhao, J. Yang, J. Hou, J. Chem. Phys. 129 (2008) 044703.
[30] M.D. Rasmussen, L.M. Molina, B. Hammer, J. Chem. Phys. 120 (2004) 988.
[31] J.P. Perdew, K. Burke, M. Ernzerhof, Phys. Rev. Lett. 77 (1996) 3865.
[32] G. Kresse, D. Joubert, Phys. Rev. B 59 (1999) 1758.
[33] P.E. Blochl, Phys. Rev. B 50 (1994) 17953.
[34] H.J. Monkhorst, J.D. Pack, Phys. Rev. B 13 (1976) 5188.
[35] P.W. Tasker, J. Phys. C 12 (1979) 4977.
[36] J.P. LaFemina, Cri. Ref. Surf. Chem. 3 (1994) 279.
[37] G. Mills, H. Jonsson, G.K. Schenter, Surf. Sci. 324 (1995) 305.
[38] S.G. Park, B. Magyari-Kope, Y. Nishi, Phys. Rev. B 82 (2010) 115109.
[39] D.J. Shu, S.T. Ge, M. Wang, N.B. Ming, Phys. Rev. Lett. 106 (2011) 039902.